VOLUME 118, NUMBER 48
DECEMBER 4, 1996

JOURNAL OF THE AMERICAN CHEMICAL SOCIETY

Design, Synthesis, and Analysis of Disulfide Cross-Linked DNA Duplexes

Scott E. Osborne,[§] Jens Völker,[‡] Shawn Y. Stevens,[§] Kenneth J. Breslauer,*[,‡] and Gary D. Glick*[,§]

Contribution from the Department of Chemistry, University of Michigan, Ann Arbor, Michigan 48109-1055, and Department of Chemistry, Rutgers University, Piscataway, New Jersey 08854

Received July 11, 1996[⊗]

Abstract: The design, synthesis, and analysis of analogs of d(CGCGAATTCGCG)$_2$ possessing one or two intrahelical disulfide cross-links is reported. The cross-linked oligomers were prepared by first synthesizing duplexes where the 3′- and 5′-terminal bases of the parent sequence were replaced with N^3-thioethylthymidine. Following deprotection and purification, air oxidation afforded the desired cross-linked constructs in high yield. Analysis of both the oxidized (disulfide cross-linked) and reduced (thiol modified) duplexes by UV, circular dichroism, and NMR spectroscopies along with susceptibility to *Eco*RI cleavage indicates that the modifications are not structurally perturbing. Optical thermal denaturation and differential scanning calorimetry measurements suggest that introducing disulfide cross-link(s) into d(CGCGAATTCGCG)$_2$ does, however, cause two fundamental changes. First, the cross-link(s) increase the thermal stability of the modified duplexes by changing the molecularity of denaturation without an increase in enthalpy. Second, the disulfide cross-link traps one of the conformations of the conformationally heterogeneous parent molecule resulting in a conformationally homogeneous system. Both of these features are themselves unique and will be important for further applications of disulfide cross-linked oligomers such as these in studies of nucleic acid structure and function.

Introduction

A range of chemical and enzymatic methods have been developed to incorporate cross-links into the helical regions of DNA and RNA.[1] Cross-linked oligonucleotides have many utilities such as models of high molecular weight DNA in thermodynamic experiments[2] and as conformationally stable constructs for molecular recognition studies.[3] Typically, cross-links are introduced by reaction of alkylating agents[4] or mutagens[5] with nucleophilic sites on the bases. Because these reagents often have little or no sequence specificity, a complex

§ University of Michigan.
‡ Rutgers University.
⊗ Abstract published in *Advance ACS Abstracts,* November 15, 1996.

(1) For examples, see: (a) Pinto, A. L.; Lippard, S. *J. Biochem. Biophys. Acta* **1985**, *780*, 167−180. (b) Borowy-Borowski, H.; Lipman, R.; Tomasz, M. *Biochemistry* **1990**, *29*, 2999−3006. (c) Kirchner, J. J.; Hopkins, P. B. *J. Am. Chem. Soc.* **1991**, *113*, 4681−4682. (d) Boger, D. L.; Munk, S. A.; Ishizaki, T. *J. Am. Chem. Soc.* **1991**, *113*, 2779−2780. (e) Sigurdsson, S. T.; Rink, S. M.; Hopkins, P. B. *J. Am. Chem. Soc.* **1993**, *115*, 12633−12634. (f) Willis, M. C.; Hicke, B. J.; Uhlenbeck, O. C.; Cech, T. R.; Koch, T. H. *Science* **1993**, *262*, 1255−1257.

(2) (a) Erie, D.; Sinha, N.; Olson, W.; Jones, R.; Breslauer, K. *Biochemistry* **1987**, *26*, 7150−7159. (b) Erie, D. A.; Jones, R. A.; Olson, W. K.; Sinha, N. K.; Breslauer, K. J. *Biochemistry* **1989**, *28*, 268−273. (c) Doktycz, M. J.; Goldstein, R. F.; Paner, T. M.; Gallo, F. J.; Benight, A. S. *Biopolymers* **1992**, *32*, 849−864.

(3) (a) Ma, M. Y.-X.; McCallum, K.; Climie, S. C.; Kuperman, R.; Lin, W. C.; Sumner-Smith, M.; Barnett, R. W. *Nucleic Acids Res.* **1993**, *21*, 2585−2589. (b) Ma, M. Y.-X.; Reid, L. S.; Climie, S. C.; Lin, W. C.; Kuperman, R.; Sumner-Smith, M.; Barnett, R. W. *Biochemistry* **1993**, *32*, 1751−1758. (c) Stevens, S. Y.; Swanson, P. C.; Voss, E. W., Jr.; Glick, G. D. *J. Am. Chem. Soc.* **1993**, *115*, 1585−1586.

(4) Millard, J. T.; Raucher, S.; Hopkins, P. B. *J. Am. Chem. Soc.* **1990**, *112*, 2459−2460.

S0002-7863(96)02386-4 CCC: $12.00

mixture of adducts is often produced.[6] Although natural products like mitomycin C[1b,7] and cisplatin[8] form lesions at unique sites, these reagents require specific recognition sequences to be present within a target duplex to generate the cross-link thereby limiting their utility. In some cases, cross-link formation by natural products can also disrupt base stacking.[4,8a]

An alternative approach for preparing cross-linked nucleic acids is to site-specifically place reactive functional groups in proximity on opposing strands of a duplex.[9] These cross-links are generally designed to occupy the sterically accessible space of either the major or minor groove. For example, Cowart and Benkovic replaced 2′-deoxyguanosine with N^6,N^6-ethano-2,6-diaminopurine on a 13-base single stranded DNA primer.[9a,10] Upon annealing to a template, attack by the cytosine N^4 atom complementary to the modification selectively opens the aziridine to form the cross-link. More recently, Verdine's group demonstrated that placing thioalkyl derivatives of either 2′-deoxyadenosine or 2′-deoxycytosine in consecutive base-pairs on opposite strands of a duplex affords disulfide cross-links under oxidative conditions.[9d,11] These cross-links impart increased stability to DNA, apparently with minimal distortion of native geometry.

Although cross-links positioned within the grooves of duplex DNA are valuable tools, such modifications can have several drawbacks. For example, by occupying either the major or minor groove, protein and drug binding may not be possible since the cross-link could sterically occlude recognition.[12] Moreover, cross-links in the grooves may alter the hydration state of the DNA which could effect the overall stability of the structure in question.[13] An alternative approach is to cross-link the terminus of a duplex where modifications should interfere less with ligand recognition and hydration. For example, several groups have cross-linked the terminal 3′- and 5′-hydroxyl groups with tethers like (oligo)ethylene glycol or (oligo)nucleotides.[2,14] However, it is not easy to end-label these structures,[15] which can restrict the utility of such oligonucleotides for studying both protein and drug binding. In addition, glycol cross-links can disrupt native geometry.[14g]

Due to the advantages associated with cross-link formation at the terminus of nucleic acid duplexes, we decided to modify positions other than the terminal hydroxyl groups. In designing our cross-link we exploited the fact that the terminal bases in duplexes have a reduced stability due to end-effects, often referred to as "end fraying".[16] Therefore, chemically modifying the hydrogen bonding groups of opposing bases at oligonucleotide termini should have a limited influence on the stability of duplexes[17] provided that the modification does not significantly disrupt base stacking. We selected to use disulfide bonds to form the cross-link because disulfide bonds are formed in high yield, are stable to wide array of solvents and reagents, the chemical reversibility available through reduction will allow for physical analysis of the modified structures before and after the cross-link is formed, and disulfide cross-linked nucleic acids are in fact well-known.[18]

In several preliminary communications, we have demonstrated that disulfide cross-links can be site-specifically incorporated at the helical termini of various DNA secondary structures.[19] As with any nucleic acid modification, a comprehensive understanding of the chemical and biological consequences of incorporating our cross-link is needed for broad application of this chemistry. Hence, we report the synthesis and analysis of disulfide cross-linked analogs of the Dickerson/Drew dodecamer, d(CGCGAATTCGCG)$_2$.[20] As part of this work we present the first use of calorimetry to elucidate, rigorously, the thermodynamic consequences of constraining DNA with disulfide cross-links.

Results

Design and Synthesis. The design of our disulfide cross-link has been described previously.[19a] Briefly, molecular modeling studies indicate that a six-atom carbon linker can span the N^3 positions of two opposing thymidine residues. If this "mismatch" is at the terminus of a duplex, the linker can be accommodated beneath the helix and should not disrupt structure/base-pairing of the adjacent residues. Therefore, to cross-link these N^3 positions we synthesized N^3-thioethylthymidine (**T*$_{SH}$**). Using automated solid-phase DNA synthesis, we have incorporated **T*$_{SH}$** at both the 3′- and 5′-ends of oligonucleotides, and under oxidative conditions, the thiol groups react to afford disulfide cross-links.[19] We chose to explore the properties of such cross-linked DNA constructs by

(5) Kirchner, J. J.; Sigurdsson, S. T.; Hopkins, P. B. *J. Am. Chem. Soc.* **1992**, *114*, 4021−4027.

(6) Millard, J. T.; Weidner, M. F.; Kirchner, J. J.; Ribeiro, S.; Hopkins, P. B. *Nucleic Acids Res.* **1991**, *19*, 1885−1891.

(7) (a) Tomasz, M.; Lipman, R.; Chowdary, D.; Pawlak, J.; Verdine, G. L.; Nakanishi, K. *Science* **1987**, *235*, 1204−1208. (b) Teng, S. P.; Woodson, S. A.; Crothers, D. M. *Biochemistry* **1989**, *28*, 3901−3907.

(8) (a) Sherman, S. E.; Gibson, D.; Wang, A. H. J.; Lippard, S. J. *Science* **1985**, *230*, 412−417. (b) Lemaire, M.-A.; Schwartz, A.; Rahmouni, A. R.; Leng, M. *Proc. Natl. Acad. Sci. U.S.A.* **1991**, *88*, 1982−1985.

(9) For examples, see: (a) Cowart, M.; Benkovic, S. J. *Biochemistry* **1991**, *30*, 788−796. (b) Milton, J.; Connolly, B. A.; Nikiforov, T. T.; Cosstick, R. *J. Chem. Soc., Chem. Commun.* **1993**, 779−780. (c) Ferentz, A. E.; Keating, T. A.; Verdine, G. L. *J. Am. Chem. Soc.* **1993**, *115*, 9006−9014 and references therein. (d) Erlanson, D. A.; Chen, L.; Verdine, G. L. *J. Am. Chem. Soc.* **1993**, *115*, 12583−12584.

(10) (a) Cowart, M.; Gibson, K. J.; Allen, D. J.; Benkovic, S. J. *Biochemistry* **1989**, *28*, 1975−1983. (b) Catalano, C. E.; Benkovic, S. J. *Biochemistry* **1989**, *28*, 4374−4382.

(11) (a) MacMillan, A. M.; Verdine, G. L. *J. Org. Chem.* **1990**, *55*, 5931−5933. (b) Ferentz, A. E.; Verdine, G. L. *J. Am. Chem. Soc.* **1991**, *113*, 4000−4002.

(12) (a) Zimmer, C.; Wähnert, U. *Prog. Biophys. Molec. Biol.* **1986**, *47*, 31−112. (b) Neidle, S. *FEBS Lett.* **1992**, *298*, 97−99.

(13) (a) Subramanian, P. S.; Ravishanker, G.; Beveridge, D. L. *Proc. Natl. Acad. Sci. U.S.A.* **1988**, *85*, 1836−1840. (b) Subramanian, P. S.; Swaminathan, S.; Beveridge, D. L. *J. Biomol. Struct. Dyn.* **1990**, *7*, 1161−1165.

(14) (a) Durand, M.; Chevrie, K.; Chassignol, M.; Thuong, N. T.; Maurizot, J. C. *Nucleic Acids Res.* **1990**, *18*, 6353−6359. (b) Kool, E. T. *J. Am. Chem. Soc.* **1991**, *113*, 6265−6266. (c) Ashley, G. W.; Kushlan, D. M. *Biochemistry* **1991**, *30*, 2927−2933. (d) Rumney, S. IV; Kool, E. T. *Angew. Chem., Int. Ed. Engl.* **1992**, *31*, 1617−1619. (e) Salunkhe, M.; Wu, T.; Letsinger, R. L. *J. Am. Chem. Soc.* **1992**, *114*, 8768−8772. (f) Bannwarth, W.; Dorn, A.; Iaiza, P.; Pannekouke, X. *Helv. Chim. Acta* **1994**, *77*, 182−193. (g) Gao, H.; Chidambaram, N.; Chen, B. C.; Pelham, D. E.; Patel, R.; Yang, M.; Zhou, L.; Cook, A. Cohen, J. S. *Bioconjugate Chem.* **1994**, *5*, 445−453. (h) Gao, H.; Yang, M.; Cook, A. F. *Nucleic Acids Res.* **1995**, *23*, 285−292.

(15) [^{32}P] can be incorporated during the ligation reaction,[3,14h] however, this procedure requires substantially more DNA, enzyme, and [^{32}P] labeled ATP than traditional end-labeling protocols.

(16) Patel, D. J.; Hilbers, C. W. *Biochemistry* **1975**, *14*, 2651−2656.

(17) For example, the free energy of a dT·dT mismatch located at the terminus of a duplex is approximately 1.0 kcal/mol more stable than a dT·dT mismatch within a duplex: (a) Aboul-ela, F.; Koh, D.; Tinoco, I., Jr. *Nucleic Acids Res.* **1985**, *13*, 4811−4824. (b) Freier, S. M.; Kierzek, R.; Caruthers, M. H.; Neilson, T.; Turner, D. H. *Biochemistry* **1986**, *25*, 3209−3213.

(18) (a) Lipsett, M. N. *Cold Spring Harb. Symp. Quant. Biol.* **1966**, *31*, 449−455. (b) Lipsett, M. N.; Doctor, B. P. *J. Biol. Chem.* **1967**, *242*, 4072−4077. (c) Lipsett, M. N. *J. Biol. Chem.* **1967**, *242*, 4067−4071.

(19) (a) Glick, G. D. *J. Org. Chem.* **1991**, *56*, 6746−6747. (b) Glick, G. D.; Osborne, S. E.; Knitt, D. S.; Marino, J. P., Jr. *J. Am. Chem. Soc.* **1992**, *114*, 5447−5448. (c) Goodwin, J. T.; Glick, G. D. *Tetrahedron Lett.* **1994**, *35*, 1647−1650. (d) Goodwin, J. T.; Osborne, S. E.; Swanson, P. C.; Glick, G. D. *Tetrahedron Lett.* **1994**, *35*, 4527−4530.

(20) (a) Wing, R.; Drew, H.; Takano, T.; Broka, C.; Tanaka, S.; Itakura, K.; Dickerson, R. E. *Nature* **1980**, *287*, 755−758. (b) Drew, H. R.; Dickerson, R. E. *J. Mol. Biol.* **1981**, *151*, 535−556.

Scheme 1. Synthesis of *tert*-Butyl Protected (**T*$_{tBu}$**) Mononucleosides (Bz = benzoyl; DMTr = 4,4′-dimethoxytrityl; CPG = controlled pore glass)[a]

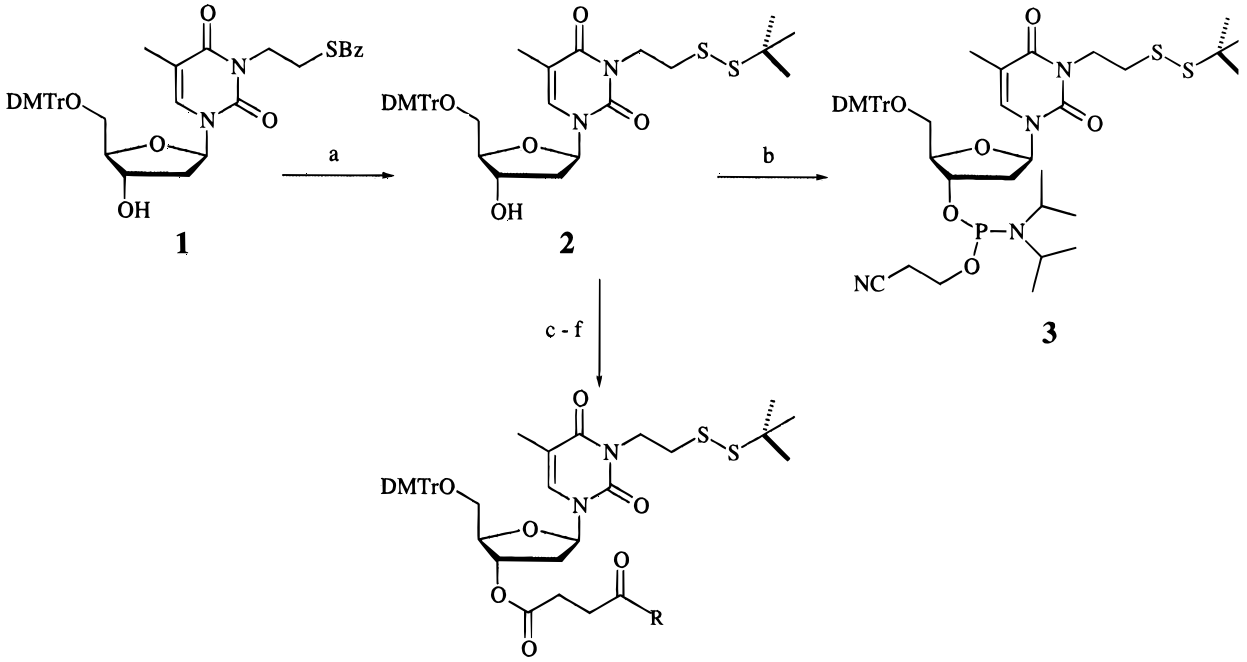

1 **2** **3**

4; R = OH

5; R = O*p*-NO_2Bz

6; R = NH-CPG

[a] (a) 1-(*tert*-butylthio)-1,2-hydrazinedicarboxmorpholide,[27] LiOH·H_2O, CH_3OH, THF (79% yield); (b) *N*,*N*-diisopropylethylamine, CH_2Cl_2, Chloro-*N*,*N*-diisopropylamino-β-cyanoethylphosphine (71% yield); (c) 4-(dimethylamino)pyridine, pyridine, succinic anhydride (76% yield); (d) CH_2Cl_2, *N*,*N*-dicyclohexylcarbodiimide, *p*-nitrophenol (59% yield); (e) CPG (500 Å, 120/200 mesh, 100.1 μmol/g), DMF, Et_3N; (f) pyridine, 4-(dimethylamino)pyridine, acetic anhydride (loading concentration of 33 μmol/g).

synthesizing analogs of d(CGCGAATTCGCG)$_2$ because the structure, thermodynamic stability, and *in vitro* biological activity of this dodecamer are very well-established.[20−21]

In initial studies we protected the thiol group on **T*$_{SH}$** with a benzoyl group for solid-phase DNA synthesis since it can be removed under conditions used to cleave the DNA from the solid support and an extra deprotection step would not be required. However, additional exposure to NH_4OH for 7 h at 55 °C, which removes the *N*-benzoyl and *N*-isobutyryl base-protecting groups,[22] leads to degradation of the thiols. Although this degradation could be partially suppressed using rapid deprotecting amidites,[23] base deprotection still resulted in low yields of product due to degradation of the thiol linker. Several laboratories have reported that mixed disulfides can be used to protect thiol groups during solid-phase DNA synthesis.[24] These mixed disulfides remain intact during base deprotection and can be removed by mild reduction. Therefore, we protected the thiol group on **T*$_{SH}$** as a *tert*-butyl mixed disulfide (**T*$_{tBu}$**) and found that this protecting group is stable to all conditions of solid-phase synthesis, deprotection, and purification.[25−26] In addition, with this new strategy standard *N*-benzoyl and *N*-isobutyryl base protected amidites can be used.

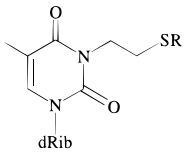

T*$_{SH}$; R = H

T*$_{tBu}$; R = StBu

T*$_2$; R = $_2$

Synthesis of the *tert*-butyl protected monomers was conducted on multigram scale in high yield (Scheme 1). Briefly, the N^3-thiobenzoyl thymidine (**1**) was prepared as previously described by Glick[19a] and was then converted to the *tert*-butyl mixed disulfide **2** using 1-(*tert*-butylthio)-1,2-hydrazinedicarboxmor-

(21) (a) Patel, D. J.; Kozlowski, S. A.; Marky, L. A.; Broka, C.; Rice, J. A.; Itakura, I.; Breslauer, K. J. *Biochemistry* **1982**, *21*, 428−436. (b) Hare, D. H.; Wemmer, D. E.; Chou, S.-H.; Drobny, G.; Reid, B. R. *J. Mol. Biol.* **1983**, *171*, 319−336. (c) Marky, L. A.; Blumenfeld, K. S.; Kozlowski, S.; Breslauer, K. J. *Biopolymers* **1983**, *22*, 1247−1257. (d) Ott, J.; Eckstein, F. *Biochemistry* **1985**, *24*, 2530−2535. (e) Nerdal, W.; Hare, D. R.; Reid, B. R. *Biochemistry* **1989**, *28*, 10008−10021.

(22) McBride, L. J.; Kierzek, R.; Beaucage, S. L.; Caruthers, M. H. *J. Am. Chem. Soc.* **1986**, *108*, 2040−2048.

(23) (a) Vu, H.; McCollum, C.; Jacobson, K.; Theisen, P.; Vinayak, R.; Spiess, E.; Andrus, A. *Tetrahedron Lett.* **1990**, *31*, 7269−7272. (b) Sinha, N. D.; Davis, P.; Usman, N.; Pérez, J.; Hodge, R.; Kremsky, J.; Casale, R. *Biochimie* **1993**, *75*, 13−23.

(24) For example, see: (a) Zuckermann, R.; Corey, D.; Schultz, P. G. *Nucleic Acids Res.* **1987**, *15*, 5305−5321. (b) Gupta, K. C.; Sharma, P.; Sathyanarayana, S.; Kumar, P. *Tetrahedron Lett.* **1990**, *31*, 2471−2474.

(25) Goodwin, J. T.; Glick, G. D. *Tetrahedron Lett.* **1993**, *34*, 5549−5552.

(26) For reviews of solid-phase oligonucleotide chemistry and synthesis, see: (a) Beaucage, S. L.; Caruthers, M. H. *Tetrahedron Lett.* **1981**, *22*, 1859−1862. (b) Gough, G. R.; Brunden, M. J.; Gilham, P. T. *Tetrahedron Lett.* **1981**, *22*, 4177−4180. (c) Adams, S. P.; Kavka, K. S.; Wykes, E. J.; Holder, S. B.; Galluppi, G. R. *J. Am. Chem. Soc.* **1983**, *105*, 661−663. (d) Caruthers, M. H.; Barone, A. D.; Beaucage, S. L.; Dodds, D. R.; Fisher, E. F.; McBride, L. J.; Matteucci, M.; Stabinsky, Z.; Tang, J.-Y. *Methods Enzymol.* **1985**, *154*, 287−313. (e) Caruthers, M. H. *Acc. Chem. Res.* **1991**, *24*, 278−284.

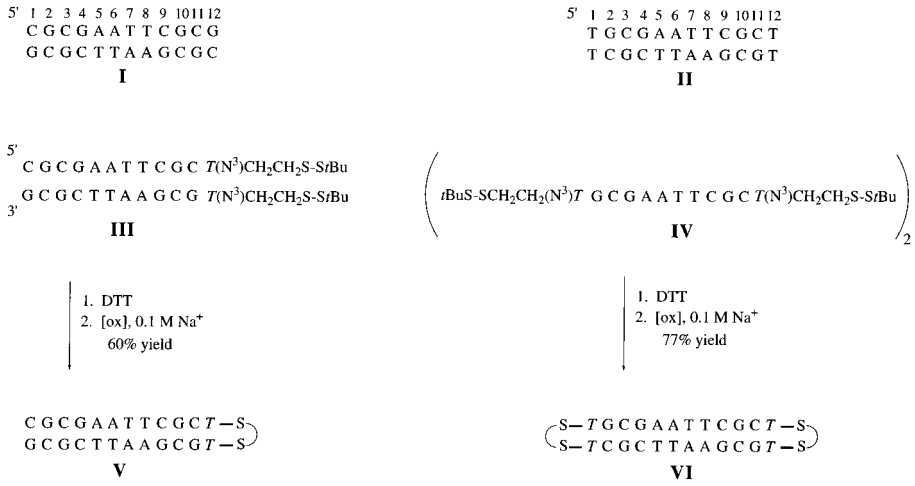

Figure 1. Synthesis of the thiol/disulfide modified oligomers. Duplexes III and IV were purified by reversed-phase HPLC before and after detritylation. Incorporation of $\mathbf{T^*_{tBu}}$ and $\mathbf{T^*_2}$ was confirmed by polyacrylamide gel electrophoresis and enzymatic nucleoside composition analysis as previously described.[19b] Sequence III requires the annealing of two non-self-complementary strands whereas the self-complementary sequence IV spontaneously anneals to form duplex DNA. Yields reported are from the *tert*-butyl protected oligonucleotides to the isolated cross-linked sequences (the cross-linking reaction was near quantitative by HPLC). Numbering for the duplexes refers to base-pair from the 5′-end shown explicitly.

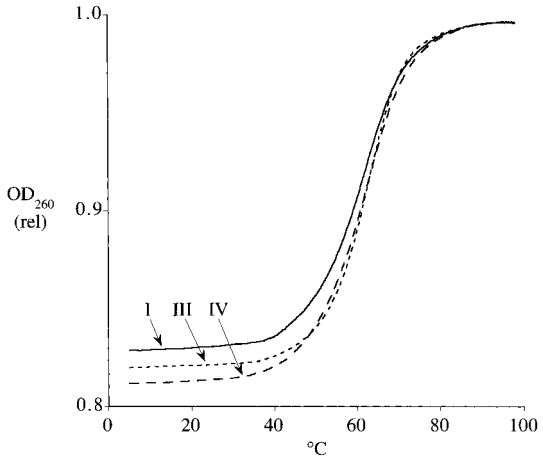

Figure 2. UV thermal denaturation curves of I, III, and IV measured in 0.1 M NaCl, 1 mM NaH_2PO_4, and 0.1 mM EDTA buffer, pH 7.0 and [DNA] = 50 μM. Melting temperatures (°C) are 61.2 for I; 62.2 for III; and 61.5 for IV.

pholide.[27] Preparation of oligonucleotides containing $\mathbf{T^*_{tBu}}$ at the 5′-terminus was accomplished by activation of the 3′-hydroxyl as the *N,N*-diisopropyl-β-cyanoethyl phosphoramidite (**3**). For sequences that require $\mathbf{T^*_{tBu}}$ at the 3′-terminus, the 3′-hydroxyl group on **2** was attached to controlled-pore glass (CPG; **6**) via a succinate linker. Loading of **6** on CPG is usually 33 μmol/g as determined by trityl cation release assay.[28]

Synthesis of the $\mathbf{T^*_{tBu}}$ containing dodecamers (sequences III and IV) was achieved via automated solid-phase DNA synthesis using standard coupling protocols with average stepwise coupling efficiencies >98.5% (Figure 1).[26] Following isolation and purification of the *tert*-butyl protected dodecamers, optical melting experiments were performed to determine whether the thiol modification affects the stability of the duplex relative to the parent dodecamer (Figure 2). Replacement of one or both of the terminal dG·dC bases of $d(CGCGAATTCGCG)_2$ with $\mathbf{T^*_{tBu}}$·$\mathbf{T^*_{tBu}}$ does not significantly alter the thermal stability or shape of the UV melting transition relative to the wild-type dodecamer. These data indicate that changes in solution conditions to enhance the stability of the modified duplexes (i.e., [Na^+], temperature, [DNA], or pH) prior to oxidative cross-linking are not required. Thermal denaturation of the dodecamers containing $\mathbf{T^*_{SH}}$ (the reduced forms of III and IV) under anaerobic conditions affords UV curves and melting temeratures (T_m) that are similar to the corresponding *tert*-butyl analogs (data not shown). Because sequences containing $\mathbf{T^*_{tBu}}$ cannot oxidatively cross-link, they are easier to manipulate and were used as a model for the reduced dodecamers in the remaining studies.

Synthesis of cross-linked duplexes V and VI was conducted by first removing the thiol protecting groups from III and IV, respectively, with dithiothreitol (DTT). After purification by reversed-phase high performance liquid chromatography (HPLC), the reduced oligonucleotides were dissolved in phosphate buffer and stirred vigorously while exposed to air at room temperature for 18 h to effect air oxidation of the thiol groups (Figure 1). The cross-linked products were then purified by reversed-phase HPLC to give V and VI in ~45% isolated overall yield (based on a 1 μmol synthesis). Nucleoside composition analysis confirmed incorporation of the disulfide cross-link(s). Analysis by native and denaturing polyacrylamide gel electrophoresis (PAGE) indicated that the structures formed were the requisite monomeric duplexes (data not shown).[19b]

Chemical Stability. Reduction of the disulfide bond(s) in $\mathbf{T^*_{tBu}}$, $\mathbf{T^*_2}$, IV, and VI was examined using DTT and β-mercaptoethanol (BME). The apparent half-lives for reduction of $\mathbf{T^*_{tBu}}$ and $\mathbf{T^*_2}$ using DTT (5.0 mM, 125 equiv, pH 8.3, 25 °C) are 85 and <1 min, respectively, whereas the apparent half-lives for reduction of sequences IV and VI are 270 min and 32 min, respectively. The slower reduction rate for $\mathbf{T^*_{tBu}}$ relative to $\mathbf{T^*_2}$ probably results from steric hindrance presented by the *tert*-butyl group. The decrease in reactivity for the DNA oligomers relative to the protected mononucleosides may arise from electrostatic repulsion between the thiolate anion on the reductant[29] and the phosphate groups proximal to the modified thymidines.[30] This hypothesis is supported by the observation that the cross-linked oligomers that are phosphorylated at the 5′-terminus are significantly more resistant to reduction (data

(27) (a) Bock, H.; Kroner, J. *Chem. Ber.* **1966**, *99*, 2039−2051. (b) Wünsch, E.; Moroder, L.; Romani, S. *Hoppe-Seyler's Z. Physiol. Chem.* **1982**, *363*, 1461−1464.

(28) Schaller, H.; Weimann, G.; Lerch, B.; Khorana, H. G. *J. Am. Chem. Soc.* **1963**, *85*, 3821−3827.

(29) The pK_a of DTT and BME are 8.9 and 9.5, respectively, at 25 °C: *Lange's Handbook of Chemistry*; Dean, J. A., Ed.; McGraw-Hill: New York, 1992; p 8.39.

(30) Snyder, G. H.; Reddy, M. K.; Cennerazzo, M. J.; Field, D. *Biochim. Biophys. Acta* **1983**, *749*, 219−226.

Table 1. Reduction of VI Using DTT

	[reductant], mM	$t_{1/2}$ pH 7.0,[a] min	$t_{1/2}$ pH 8.3,[a] min
DTT	0.1	>24 h	>24 h
	5	82	40
	10	72	15
	15	55	5
BME	5	>24 h	>24 h
	50	270	43
	100	50	6
	200	15	3

[a] Error in the apparent half-lives is ±10%.

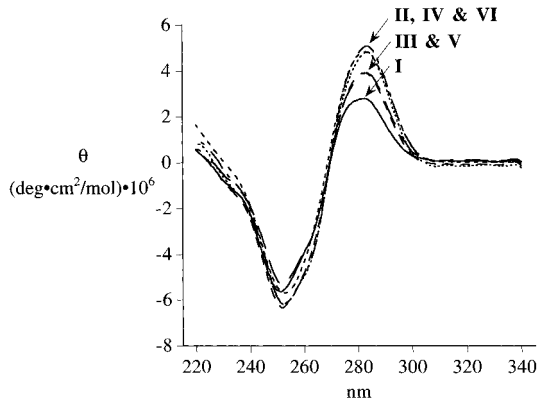

Figure 3. Circular dichroism curves of I−VI measured in 0.1 M NaCl, 1 mM NaH_2PO_4 and 0.1 mM EDTA buffer, pH 7.0 and [DNA] = 20 μM. Data points were normalized from millidegrees to θ according to DNA concentration.

not shown). The smaller difference in the rate of reduction between IV and VI versus **T*$_{tBu}$** and **T*$_2$** (e.g., 8.5- versus 85-fold, respectively) is probably steric in origin.

At low concentrations of DTT (0.1 mM) or BME (5 mM), the disulfide cross-link in VI appears to remain intact for 24 h, either at pH 7.0 or at 8.3 (Table 1). Increasing the concentration of either reductant (5−15 mM DTT and 50−200 mM BME), leads to a decrease in the apparent half-life of the cross-link. When the pH is decreased from 8.3 to 7.0, the disulfide bond is between 2- and 12-fold more resistant to reduction. The apparent resistance to reduction of the cross-link at low concentrations of either DTT or BME is probably due to competitive reoxidation of the dodecamer rather than direct resistance to the reductant.[31] Indeed, if the reduction is allowed to proceed for several days (regardless of starting reductant concentration), only the cross-linked structure remains which presumably results from the depletion of all reductant. The increase in resistance to reduction with lower pH is due to the smaller percentage of thiolate present under neutral conditions.[29]

Structural Analysis: Circular Dichroism (CD). CD spectroscopy was used to study the macroscopic helical geometry of the chemically modified oligomers. The wild-type dodecamer displays a characteristic B-DNA spectrum possessing a positive ellipticity at 283 nm, a negative ellipticity at 252 nm, and a crossover at 269 nm (Figure 3).[32] Sequences III and V which contain the thiol-modified thymidines at one end of the helix afford the same spectral pattern as I but with higher positive amplitude at 283 nm. Duplexes IV and VI possessing the modification at both ends display a greater increase in positive amplitude at 283 nm without any other significant changes in the overall CD spectrum relative to I. To understand the origin of the increased elliptic signal at 283 nm, we replaced the terminal dG·dC bases on I with dT (Sequence II). The CD

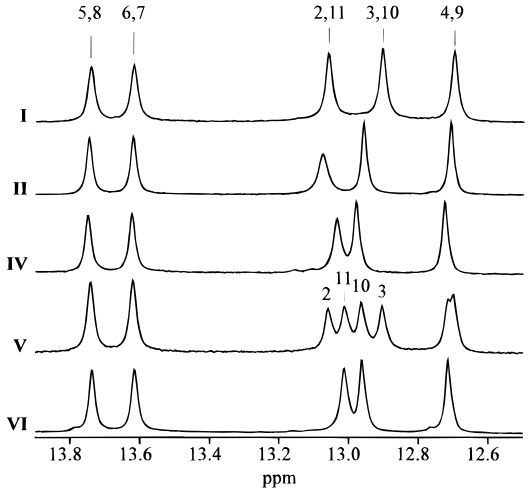

Figure 4. ^{1}H NMR imino proton spectra of I, II, IV, V, and VI at 30 °C in phosphate buffer (10 mM NaH_2PO_4, pH 7.0 and [DNA] = 2 mM). Numbering for each imino proton resonance refers to base-pair from the 5′-end shown explicitly in Figure 1.

spectrum of II is nearly superimposible with IV and VI suggesting that the small differences in the CD spectra may simply arise from the inherent differences in the composition of the sequences.[33] It is also possible that the increase in ellipticity at 283 nm may be related to an increased winding of the helix induced by the presence of the thymidine bases.[34] Regardless, the general correspondence in the CD curves suggests that the terminal base modifications do not significantly distort the helical geometry of the duplex relative to I and there appears to be no helical differences between the *tert*-butyl protected sequences and their cross-linked counterparts.

Structural Analysis: NMR. The ^{1}H NMR spectra of sequences I, IV, and VI measured at 30 °C in H_2O/D_2O each show five imino proton resonances (Figure 4). By contrast, V is not C2-symmetric so that eight imino proton resonances are observed (the dA·dT base-pairs are not resolved at 500 MHz). These signals, along with the nonlabile proton resonances, were assigned using NOESY spectra as previously described.[21e] The chemical shift values for the imino proton resonances in IV and VI are within 0.07 ppm of the corresponding signals for the wild-type dodecamer.[21a] The small differences in chemical shift relative to I may result from structural changes imparted by the disulfide cross-link or from the inherent differences in the base composition. To distinguish between these possibilities, we examined II. As seen in Figure 4, the imino proton spectrum of II resembles the spectra of IV and VI more closely than the spectrum of I ($\Delta\delta$ < 0.04 ppm). These data suggest that the spectral differences in the imino proton region result mainly from local anisotropy changes associated with different base-stacking patterns between the terminal and penultimate bases which is consistent with the UV and CD data.

A thermal melting study monitoring the imino protons was conducted to determine how the terminal modification(s) affects end-fraying and denaturation of these dodecamers. Denaturation of I, II, and V begins with fraying of the terminal base-pairs at 10 °C, then proceeds sequentially toward the center of the helix (data not shown). After the second base-pair has denatured, there is rapid melting of the central region. The imino protons for sequences IV and VI appear to melt along pathways similar to the wild-type dodecamer: the central dA·dT base-pairs exhibit

(31) A similar observation has been made by Ferentz *et al.*[9c]

(32) Ivanov, V. I.; Minchenkova, L. E.; Schyolkina, A. K.; Poletayev, A. I. *Biopolymers* **1973**, *12*, 89−110.

(33) Amaratunga, M.; Snowden-Ifft, E.; Wemmer, D. E.; Benight, A. S. *Biopolymers* **1992**, *32*, 865−879.

(34) Baase, W. A.; Johnson, W. C., Jr. *Nucleic Acids Res.* **1979**, *6*, 797−814.

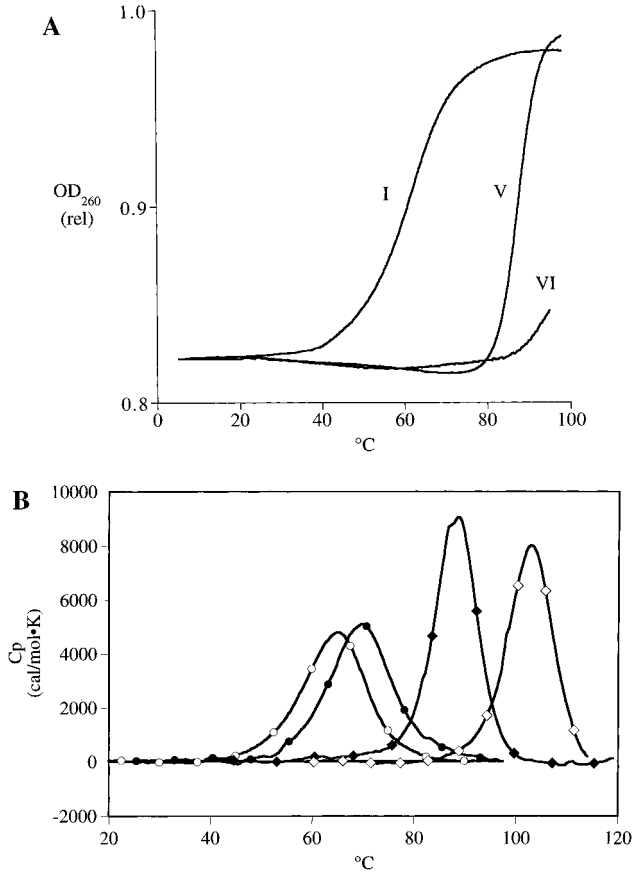

Figure 5. Optical and DSC data. (A) UV thermal denaturation curves of I, V, and VI measured in 0.1 M NaCl, 1 mM NaH_2PO_4 and 0.1 mM EDTA buffer, pH 7.0 and [DNA] = 50 μM. Sequences V and VI melt in a concentration independent manner, indicating that the molecularity has been reduced from bimolecular to monomolecular (data not shown). Similar data was obtained at lower scan rates (0.2 °C/min) and hysteresis was not observed for any of the sequences studied. Melting temperatures (°C) are 61.2 for I; 87.8 for V; and > 95 for IV. (B) DSC curves of I (○), II (●), V (◆), and VI (◇) measured in 0.1 M NaCl, 10 mM NaH_2PO_4 and 0.1 mM EDTA buffer, pH 7.0 at the concentrations listed in Table 2. The calorimetric van't Hoff values agree within 5% of the optically determined values.

a linear change in chemical shift with temperature and the imino resonances of the third and fourth dG·dC base-pairs do not display a temperature dependence below 30 °C. Similar imino melting spectra for I and related sequences have been observed which suggests that the base modifications do not disrupt the local dynamics of the dodecamer.[21a,35] Although sequence V also displays a similar melting profile, this spectrum is difficult to analyze due to the loss of C2-symmetry and significant resonance overlap.

Thermal and Thermodynamic Stability. UV and differential scanning calorimetry (DSC) measurements were conducted to characterize the thermally-induced denaturation of duplexes I−VI with the specific goal of elucidating the thermal and thermodynamic consequences of modifying and constraining DNA via our disulfide chemistry.[36] The results of these studies are shown in Figures 2 and 5, with the associated data listed in Table 2. Comparing the calorimetrically determined T_m values for (mono)cross-linked duplex V (87.8 °C) and for the unconstrained duplexes I and II (70.0 and 64.4 °C, respectively)

(35) Patel, D. J.; Pardi, A.; Itakura, K. *Science* **1982**, *216*, 581−590.

(36) DSC and UV measurements indicate that III and IV have a greater propensity to adopt a hairpin structure relative to I and II. Therefore, these sequences are less useful than I and II in helping to estimate the increase on thermal stability of the cross-linked DNAs.

Table 2. Thermodynamic Values Obtained from DSC Experiments Performed in 0.1 M NaCl, 10 mM NaH_2PO_4, and 0.1 mM EDTA Buffer at pH 7.0

sequence	C_t,[a] mM	T_m[b]	ΔH_{cal}[b]	ΔH_{vH}[b]	ΔS_{cal}[b]	$\Delta H_{vH}/\Delta H_{cal}$
I	0.2608	70.0	85.4	56.0	248.9	0.66
II	0.2558	64.4	79.0	54.1	234.1	0.68
V	0.2444	87.8	98.9	97.7	274.0	0.99
VI	0.2545	102.5	95.3	96.9	253.7	1.02

[a] DNA concentrations are for the double-stranded (initial) state. [b] T_m values are in °C, and the error is ±1 °C; ΔH_{cal} and ΔH_{vH} values are in kcal/mol, and the error is ±5%; values of ΔS_{cal} are in eu and the error is ±5%.

reveals that a single disulfide cross-link results in a dramatic increase in thermal stability. By accounting for the differences in composition between I (two terminal dG·dC base pairs), II (two terminal dT·dT mismatches), and V (one terminal dG·dC base pair and one terminal modified dT·dT mismatch), we estimate that a single disulfide cross-link results in an increase in thermal stability of roughly 20 °C. Introducing a second disulfide cross-link into V to form the (bis)cross-linked duplex results in a further increase in thermal stability from 87.8 °C to 102.5 °C (ΔT_m = 14.7 °C). Accounting for the difference in composition between V and VI, we estimate that the second disulfide cross-link induces a further increase in thermal stability of 17.5 °C. Thus, the two disulfide cross-links result in a net overall thermal stabilization of 38.1 °C (64.4 °C for II versus 102.5 °C for VI). These T_m changes are particularly noteworthy considering that our NMR, CD, and *Eco*RI (*vide infra*) structural studies suggest no significant change in secondary structure is induced by the cross-link.

Duplexes I and II thermally denature in a bimolecular reaction to form two single strands. As a consequence, melting of I and II is dependent on the overall oligonucleotide concentration. In contrast, V and VI melt in a concentration independent monomolecular manner, with V denaturing to a single stranded state, while VI denatures to a conformationally constrained ring. To estimate how much of the observed ΔT_m difference results from this change in molecularity, one can "correct" for the concentration dependence of the T_m in the bimolecular duplexes following the general procedure outlined by Marky and Breslauer.[37] Specifically, "reduced" concentration independent T_m values can be estimated by extrapolating $1/T_m$ versus $\ln C_t$ plots to 1 M strand concentration (actually 1 M activity), or alternatively by simply rearranging the corresponding van't Hoff equation for bimolecular processes. Using the latter approach and our calorimetrically determined enthalpies, we estimate a reduced concentration independent T_m of 94 and 90 °C for I and II, respectively. These "reduced" T_m values are quite close to the T_m value observed for V which suggests that the overall impact of a single disulfide cross-link is largely due to the change in molecularity of the complex. In contrast, the observed increase in T_m due to the second disulfide cross-link in VI relative to V, most likely results from a different mechanism since these duplexes melt with the same molecularity. In fact, we show below that the increase in the T_m of VI relative to V is overwhelmingly entropic in origin, resulting primarily from the difference in the nature of the native and denatured states of V and VI.

The transition entropy for a bimolecular complex also depends on strand concentration. To correct for this concentration dependence, we used the general procedure outlined by Marky and Breslauer[37] to calculate a reduced entropy (ΔS^*) from the observed ΔS_{obs} values. Note, however, that our conclusions presented below and in the Discussion Section are not signifi-

(37) Marky, L. A.; Breslauer, K. J. *Biopolymers* **1987**, *26*, 1601−1620.

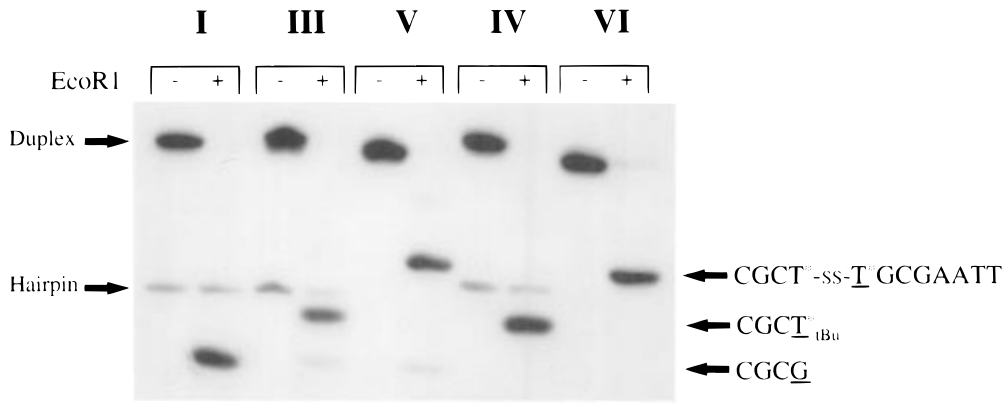

Figure 6. Autoradiogram of a 20% non-denaturing PAGE of the *Eco*RI restriction digest patterns for 5′-[^{32}P] end-labeled dodecamer sequences. Digested dodecamers I, III, and VI contain fragments that are four bases in length with the 4-mer containing $\mathbf{T^*_{tBu}}$ migrating slower on polyacrylamide gels than the unmodified 4-mer (the underlined base indicates the incorporated [^{32}P] end-label). Cross-linked sequences V and VI display a digested DNA fragment which is 12 bases in length arising from the 4-mer containing the 5′-end-label covalently attached via the disulfide cross-link to the 8-mer on the opposite strand. Note that I, III, and IV each contain a band that corresponds to the hairpin conformation which remains in equilibrium with the duplex structure. This hairpin is not cleaved by *Eco*RI.[14h] Because cleavage rates were calculated by the disappearance of the starting duplex structure, the presence of any hairpin structure should not affect the accuracy of the rate of digestion. In addition, we observe an unequal representation of the digested material in III and IV resulting from an unequal incorporation of the [^{32}P]-label at the two ends of the helix.

cantly changed by this "correction". Comparison of the calorimetrically obtained enthalpy (ΔH_{obs}) and entropy (ΔS_{obs}) values for II with those measured for V reveals a significant increase in both enthalpy ($\Delta\Delta H_{obs} = 19.9$ kcal/mol) and entropy ($\Delta\Delta S_{obs} = 40$ eu; $\Delta\Delta S^* = 23.5$ eu). By comparing the thermodynamic properties of I and II ($\Delta\Delta H_{obs} = -6.4$ kcal/mol and $\Delta\Delta S_{obs} = -15$ eu; $\Delta\Delta S^* = -15$ eu), we estimate that replacement of a single dG·dC base-pair at the terminus with thymidines results in a reduction of both enthalpy ($\Delta\Delta H_{obs} = -3.2$ kcal/mol) and entropy ($\Delta\Delta S_{obs} = -7.5$ eu; $\Delta\Delta S^* = -7.5$ eu). Consequently, after correcting for differences in the terminal base pairs of II and V, we conclude that a single disulfide cross-link contributes 16.7 kcal/mol to the enthalpy and 32.5 eu ($\Delta\Delta S^* = 16$ eu) to the entropy of the duplex. Introducing a second cross-link into the duplex (i.e., comparing V and VI), results in a small overall decrease in enthalpy ($\Delta\Delta H_{obs} = -3.6$ kcal/mol) and a more pronounced decrease in entropy ($\Delta\Delta S_{obs} = -20$ eu). Again, after "correcting" for the replacement of the terminal dG·dC base-pair with thymidines, we observe a negligible change in enthalpy ($\Delta\Delta H_{obs} = -0.4$ kcal/mol) and a larger entropic penalty ($\Delta\Delta S_{obs} = -12.5$ eu) for introducing the second disulfide cross-link. Thus, introducing two disulfide cross-links into II results in an overall enthalpy gain of 16.3 kcal/mol (ΔH_{obs}) and an entropy gain of 20 eu ($\Delta\Delta S^* = 4$ eu).

A comparison of the model dependent van't Hoff enthalpy obtained either from calorimetric melting curves or the UV data for I and II with the model independent calorimetric enthalpies reveals the van't Hoff values are considerably smaller than the corresponding calorimetric data. This disparity indicates that denaturation of duplexes I and II proceeds via a non-two-state process. This observation could reflect population of a significant fraction of partially melted duplexes. Alternatively, it is possible that some of the 12-mer exists in a competing hairpin state rather than in the duplex state. Such a concentration dependent hairpin to dimer equilibrium, in fact, previously has been observed under these solution conditions, albeit at lower oligonucleotide concentrations.[21c,38] Significantly, the van't Hoff and calorimetric data are nearly identical for V and VI which suggests that these disulfide cross-linked duplexes melt in a near two-state manner.

Nuclease Susceptibility. The class II restriction endonuclease *Eco*RI recognizes 5′-GAATTC and cleaves between the G-4:A-5 step.[39] *Eco*RI is sensitive to subtle conformational changes and has been used to probe for perturbations in B-DNA structure; i.e., a reduction in the rate of cleavage can be directly correlated to a change in helical geometry.[40] Therefore, analysis of the cleavage rates of I-VI provides another means to determine whether our modifications affect the structure of I. After 90 min, sequences I−VI are completely cleaved, producing digestion patterns unique for each sequence (Figure 6). The fact that we observe no loss in enzymatic activity for II−VI relative to I suggests that the thiol/disulfide modifications do not induce structural distortions in the parent duplex and is consistent with the UV, CD, and NMR data presented above. Inspection of the *Eco*RI digestion patterns in Figure 6 also reveals the presence of some hairpin for I, III, and IV. This hairpin is not cleaved by the enzyme and the amount of hairpin does not increase during the digestion experiment.

Cleavage by an exonuclease was also examined since the enzyme recognition site is proximal to our modified thymidines. Snake venom phophodiesterase (SVPD) degrades DNA from the 3′-end of double-stranded DNA releasing 5′-dNMPs.[41] This exonuclease degrades sequences III and IV at rates ($t_{1/2}$ of 3.8 min and 5.3 min, respectively) that are similar to that obtained for I ($t_{1/2}$ of 4.1 min, Figure 7). This result suggests that the terminal base modifications alone do not inhibit the enzyme. Placing one cross-link in the dodecamer does not alter the rate of nucleolytic digestion ($t_{1/2}$ of 5.1 min), however, when both termini are cross-linked, the apparent half-life is 500-fold greater ($t_{1/2} > 24$ h). Only when the enzyme concentration is increased

(38) (a) Wemmer, D. E.; Chou, S. H.; Hare, D. R.; Reid, B. R. *Nucleic Acids Res.* **1985**, *13*, 3755−3772. (b) Seela, F.; Kaiser, K. *Nucleic Acids Res.* **1987**, *15*, 3113−3129.

(39) (a) Frederick, C. A.; Grable, J.; Melia, M.; Samudzi, C.; Jen-Jacobson, L.; Wang, B.-C.; Greene, P.; Boyer, H. W.; Rosenberg, J. M. *Nature (London)* **1984**, *309*, 327−331. (b) Germann, M. W.; Kalisch, B. W.; Lundberg, P.; Vogel, H. J.; van de Sande, J. H. *Nucleic Acids Res.* **1990**, *18*, 1489−1498. (c) Yang, D.; Gao, Y.; Robinson, H.; van de Marel, G. A.; van Boom, J. H.; Wang, A. H.-J. *Biochemistry* **1993**, *32*, 8672−8681.

(40) (a) Alves, J.; Pingoud, A.; Haupt, W.; Langowski, J.; Peters, F.; Maass, G.; Wolff, C. *Eur. J. Biochem.* **1984**, *140*, 83−92. (b) Alves, J.; Rüter, T.; Geiger, R.; Fliess, A.; Maass, G.; Pingoud, A. *Biochemistry* **1989**, *28*, 2678−2684. (c) Wilk, A.; Koziolkiewicz, M; Grajkowski, A.; Uzanski, B.; Stec, W. J. *Nucleic Acids Res.* **1990**, *18*, 2065−2068.

(41) Williams, E. J.; Sung, S.-C.; Laskowski, M. Sr. *J. Biol. Chem.* **1961**, *236*, 1130−1134.

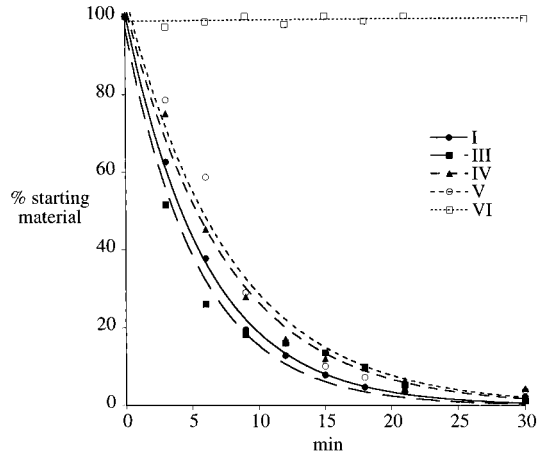

Figure 7. Exonucleolytic degradation for sequences I and III−VI. Apparent half-lives are 4.1 min for I; 3.8 min for III; 5.1 min for IV; 5.3 min for V; and >24 h for VI.

by 50-fold is appreciable cleavage observed ($t_{1/2}$ of 90 min; under these conditions the other sequences are completely degraded in < 1 min).[42] These data suggest that the nucleolytic activity may require the enzyme to partially expose the phosphodiester bonds[43] by unwinding or "melting" the helix upon binding, which is limited by the topological constraint imposed by the cross-link. Indeed, similar results have been observed by Benkovic and co-workers in the exonulcease function of the Klenow fragment for DNA polymerase I.[10]

Discussion

Although synthetic methods to prepare nucleic acids containing terminal cross-links are available, they generally possess several shortcomings. For example, in some cases the groups that form the cross-link destabilize helical structure,[2a−b,9c] and although this energetic penalty may be compensated for upon forming the cross-link, it necessarily limits the overall (thermodynamic) stability that the cross-link can provide. Also, many synthetic protocols do not yield enough purified cross-linked material for biophysical analysis like DSC, X-ray crystallography, and NMR.[2,3,14e] Furthermore, because most methods bridge the terminal hydroxyls to form the cross-link, [^{32}P]-end-labeling may be difficult to accomplish.[15]

We have designed our chemistry to address, among others, the points listed above. Specifically, our cross-link bridges functional groups on the terminal bases thereby leaving the terminal hydroxyls available for [^{32}P]-end-labeling. Disulfide bonds were chosen to form the cross-link because disulfide redox chemistry is thiol-specific, highly efficient, chemically reversible, and is precedented in the nucleic acid literature.[18,4] Although placing a cross-link between the terminal bases can disrupt Watson−Crick hydrogen bonding, this loss should be minimal due to "end-fraying" effects.[16] Moreover, our modifications should not interfere with stacking on the penultimate bases, which in general, is energetically more favorable than Watson−Crick hydrogen bonding.[17,44]

Structural Studies. The CD spectra of I−VI indicates that the global geometry of the parent duplex is not altered upon modification with $\mathbf{T^*_{tBu}}$ or $\mathbf{T^*_2}$. This conclusion is based on the fact that we observe an isobestic point at the crossover at 269 nm and no shift in the elliptic maxima at 283 nm in the spectra of II−VI relative to I. The greatest differences observed in the CD spectra of II−VI is the magnitude of the positive signal at 283 nm. This increase is apparently due to the replacement of the terminal dG·dC base-pair with thymidine bases; i.e., it is related to the differences in the composition of the various dodecamers. This hypothesis is supported by studies of DNA dumbbell sequences containing (oligo)thymidine loops where an increase in elliptic signal at 283 nm is proportional to the number of thymidines located in the loop region.[32−34]

Although NMR studies of I containing either terminal base-pair mismatches or chemical modifications of the terminal bases are not available, there are reports of variants of I containing modifications/sequence alterations within the helix.[45] For example, replacement of the dG_3·dC with mismatches like dG_3·dT, dG_3·dA, dC_3·dT, or dA_3·dC results in a shift of the imino protons proximal to the mismatch site (e.g., $\Delta\delta$ values range between 0.15−0.30 ppm).[46] These chemical shift changes relative to the corresponding resonances in I have been correlated with local structural perturbations within the helix. In contrast, Feigon *et al*. have demonstrated that the imino proton spectrum of a variant of I containing m^6dA_6·dT (which has been shown by crystallography to be structurally isomorphous to I) is nearly identical to the imino proton spectrum I ($\Delta\delta$ for each resonance are < 0.1 ppm).[47] Replacing the terminal dG·dC bases of I with either dT·dT, $\mathbf{T^*_{tBu}}$ $\mathbf{T^*_2}$, or the disulfide cross-link, leads to a small shift of the imino proton resonances proximal to the base substitution (0.07 ppm) suggesting that the base modifications do not significantly alter the native structure of I. This conclusion is also supported by the fact that (1) NOESY spectra for IV, VI, and I are quite similar[48] and (2) the NMR structures of two other constructs possessing our modification do not possess local conformational distortions proximal to the cross-link.[49]

Thermodynamic Studies. The thermodynamic characterization of I, II, and V reveals that introducing a single disulfide cross-link into the parent duplex results in a large increase in thermal and thermodynamic stability. Introducing a second disulfide cross-link into duplex V results in an additional increase in thermal stability. We have dissected the thermodynamic and extra-thermodynamic origins of the observed cross-linked induced increases in thermal stability. Upon introduction of a single disulfide cross-link, the increase in T_m can be accounted for primarily by the change in molecularity of the complex. However, if the observed change in T_m is due entirely to the molecularity of the complex, then one might expect only to observe changes in entropy. However, we observe significant changes in enthalpy in addition to entropy changes.

(42) Degradation may occur within the helix since this enzyme has an endonuclease function, albeit about 10 times slower than the exonuclease activity: Pritchard, A. E.; Kowalski, D.; Laskowski, M., Sr. *J. Biol. Chem.* **1977**, *252*, 8652−8659.

(43) Tarköy, M.; Leumann, C. *Angew. Chem., Int. Ed. Engl.* **1993**, *32*, 1432−1434.

(44) (a) Freier, S. M.; Alkema, D.; Sinclair, A; Neilson, T.; Turner, D. H. *Biochemistry*, **1985**, *24*, 4533−4539. (b) Sugimoto, N.; Kierzek, R.; Turner, D. H. *Biochemistry* **1987**, *26*, 4559−4562.

(45) (a) Miller, M.; Kirchhoff, W.; Schwarz, F.; Appella, E.; Chiu, Y.-y. H.; Cohen, J. S.; Sussman, J. L. *Nucleic Acids Res.* **1987**, *15*, 3877−3890. (b) Roongta, V. A.; Jones, C. R.; Gorenstein, D. G. *Biochemistry* **1990**, *29*, 5245−5258. (c) Borden, K. L. B.; Jenkins, T. C.; Skelly, J. V.; Brown, T.; Lane, A. N. *Biochemistry* **1992**, *31*, 5411−5422.

(46) (a) Patel, D. J.; Kozlowski, S. A.; Marky, L. A.; Rice, J. A.; Broka, C.; Dallas, J.; Itakura, K.; Breslauer, K. J. *Biochemistry* **1982**, *21*, 437−444. (b) Patel, D. J.; Kozlowski, S. A.; Ikuta, S.; Itakura, K. *Fed. Proc.* **1984**, *43*, 2663−2670. (c) Patel, D. J.; Kozlowski, S. A.; Ikuta, S.; Itakura, K. *Biochemistry* **1984**, *23*, 3207−3217. (d) Patel, D. J.; Kozlowski, S. A.; Ikuta, S.; Itakura, K. *Biochemistry* **1984**, *23*, 3218−3226.

(47) Rajagopal, P.; Gilbert, D. E.; van der Marel, G. A.; van Boom, J. H.; Feigon, J. *J. Magn. Reson.* **1988**, *78*, 526−537.

(48) Stevens, S. Y.; Glick, G. D., unpublished observations.

(49) (a) Wang, H.; Osborne, S. E.; Zuiderweg, E. R. P.; Glick, G. D. *J. Am. Chem. Soc.* **1994**, *116*, 5021−5022. (b) Wang, H.; Zuiderweg, E. R. P.; Glick, G. D. *J. Am. Chem. Soc.* **1995**, *117*, 2981−2991. (c) Cain, R. J.; Zuiderweg, E. R. P.; Glick, G. D. *Nucleic Acids Res.* **1995**, *23*, 2153−2160.

A hairpin to dimer equilibrium could account for the lower than expected enthalpy for the melting of I and II. Some hint for the origin of the enthalpy change may be found in the observation that the calorimetric enthalpies of I and II are significantly lower than the enthalpy predicted (107.8 kcal/mol) for these duplexes based on nearest neighbor data.[50] In addition, in constrast to either of the cross-linked duplexes, we observe that the model dependent van't Hoff enthalpies for I and II are significantly smaller than the corresponding calorimetric enthalpies for these duplexes. Lastly, we find that the observed enthalpy for I is somewhat smaller than the enthalpy reported in a previous study at higher oligonucleotide concentrations.[21a,c] Based on these observations and the known propensity of I to equilibrate between a hairpin and a dimer at low ionic strength and low oligonucleotide concentrations,[21c,38] we suggest that the observed low enthalpies for I and II are due primarily to the presence of a small fraction of the hairpin conformation. Based on the predicted enthalpy values for the hairpin and duplex states of I, we estimate that between 10−20% of the hairpin form would be sufficient to give rise to our calorimetric results, an amount that might be difficult to detect via optical and/or NMR measurements. However, the *Eco*RI experiments presented above reveal an extra band corresponding to the hairpin form for I and II (see Figure 6), an observation consistent with our expectations based on the thermodynamic and extra-thermodynamic data.

The disulfide cross-link appears nearly enthalpically neutral. In contrast to the bimolecular duplexes I and II, the (mono)-cross-linked duplex V and the (bis)cross-linked duplex VI reveal no evidence for hairpin to dimer equilibrium. These results suggest that the increase in enthalpy upon introducing one or two disulfide cross-links in I may simply be due to a shift in the hairpin to dimer equilibrium towards the dimer state. This reasoning is consistent with the observation that upon introducing the second disulfide cross-link we observe insignificant changes in enthalpy relative to the (mono)cross-linked sequence. This observation also suggests that the modification required to form the cross-link is essentially enthalpically neutral. Consistent with this interpretation is the fact that the measured calorimetric enthalpy for V is very close to the expected enthalpy value based on nearest neighbor interaction energies.[50]

Constraining the dodecamer by a second disulfide cross-link lowers the entropy. Experimentally, the additional increase in T_m observed on introducing the second disulfide cross-link into V is found to be almost entirely entropic in origin. The change in entropy will reflect differences in the native and/or denatured states of VI as compared to V, including differences in solvation. On first inspection, it would appear that the most likely source for the observed decrease in entropy is the denatured state, since clearly the number of conformational degrees of freedom of the denatured state of VI is less than those of V. However, the current experimental evidence cannot exclude some differential entropic contributions from the native states, as well as influences from differential solvation in both the initial and the final states. Regardless of whether the observed change is due to the native or denatured state, our data shows that the entropy term is responsible for the increase in thermal stability of VI relative to V. To our knowledge, this is the first conformationally constrained nucleic acid system where the increase in melting temperature is predominantly due to an entropy decrease.[2,14]

Conclusion

We have described the design and synthesis of disulfide cross-linked analogs of d(CGCGAATTCGCG)$_2$ and have characterized the structural, dynamic, *in vitro* biological, and thermodynamic consequences of placing our cross-links in this sequence. NMR, CD, UV, and nuclease susceptibility studies of the reduced and oxidized forms of the dodecamers show that alkylthiol modifications and the disulfide cross-link are not structurally perturbing. DSC measurements suggest that introducing cross-link(s) into I results in two fundamental changes. First, constraining the dodecamer with a disulfide cross-link results in a significant increase in thermal stability that is primarily due to entropic effects: a single disulfide cross-link changes the molecularity of the complex from bimolecular to monomolecular, while a second disulfide cross-link results in a constrained conformation with a reduced entropy. Second, the disulfide cross-link traps one of the conformations of the parent molecule resulting in a structurally homogeneous system. Collectively, our findings suggest that disulfide cross-linked oligomers such as these should be of significant utility in studies of nucleic acid structure, function, and folding.

Experimental Section

Monomer Synthesis. The general synthetic procedures employed here have been previously described.[19]

5′-*O*-(4,4′-Dimethoxytrityl)-*N*^{3}-(ethyl)thymidine *tert*-Butyl Disulfide (2). 5′-*O*-(4,4′-Dimethoxytrityl)-*N*^{3}-(thiobenzoylethyl)thymidine[19a] (**1**) and 1-(*tert*-butylthio)-1,2-hydrazinedicarboxmorpholide[27] were prepared as previously described. Compound **1** (1.01 g, 2.5 mmol) and 1-(*tert*-butylthio)-1,2-hydrazinedicarboxmorpholide (0.90 g, 2.6 mmol, 1.05 equiv) were dissolved in a MeOH/THF solution (2:1, 15.4 mL), and LiOH·H$_2$O (0.31 g, 7.4 mmol, 3 equiv) was added. The reaction mixture was stirred under N_2 for 4 h after which the solution was diluted with CH_2Cl_2 and washed with saturated sodium bicarbonate and brine. The organic layer was dried over Na_2SO_4 and concentrated under reduced pressure to give a yellow oil. The residue was chromatographed on silica gel (eluting with 25% acetone in petroleum ether) to give compound **2** (0.91 g, 79% yield) as a white foam. TLC (7.5% MeOH in CH_2Cl_2) $R_f = 0.78$. ^{1}H NMR (360 MHz, CD_3CN) δ 1.30 (9 H, s, C(C*H*$_3$)$_3$), 1.49 (3 H, s, 5-C*H*$_3$), 2.23−2.27 (2 H, m, 2′-*H*$_{a,b}$), 2.87−2.91 (2 H, m, 8-*H*$_{a,b}$), 3.26−3.28 (1 H, m, 5′-*H*$_a$), 3.36−3.38 (1 H, m, 5′-*H*$_b$), 3.75 (6 H, s, 2 OC*H*$_3$), 3.91−3.94 (1 H, m, 4′-*H*), 4.10−4.14 (2 H, m, 7-*H*$_{a,b}$), 4.42−4.49 (1 H, m, 3′-*H*), 6.26 (1 H, t, $J = 6.7$ Hz, 1′-*H*), 6.84−7.47 (14 H, m, 6-*H*, Ar*H*). ^{13}C NMR (90 MHz, CD_3CN) δ 13.0 (5-*C*H$_3$), 30.1 (C(*C*H$_3$)$_3$), 37.3 (8), 41.0 (7), 41.3 (2′), 48.4 (*C*(CH$_3$)$_3$), 55.9 (O*C*H$_3$), 64.6 (5′), 72.0 (3′), 86.1 (1′), 86.9 (4′), 87.4 (O*C*(Ph)$_3$), 110.4 (5), 114.1, 127.9, 129.0, 131.0 (Ar.), 135.2 (6), 136.7, 136.8, 146.0 (Ar.), 151.8 (2), 159.7 (Ar.), 164.1 (4). IR (KBr) 3441, 2957, 1704, 1666, 1641, 1608, 1509, 1466, 1447, 1251, 1094, 1033, 828 cm^{-1}. FAB MS (3-NBA) *m/z* 693 ($M^+ + 1$).

5′-*O*-(4,4′-Dimethoxytrityl)-*N*^{3}-(ethyl)thymidine *tert*-Butyl Disulfide 3′-*O*-((*N*,*N*-diisopropylamino-*β*-cyanoethyl)phosphoramidite) (3). Compound **2** (0.65 g, 0.94 mmol) and *N*,*N*-diisopropylethylamine (660 μL, 3.8 mmol, 4.0 equiv) were dissolved in CH_2Cl_2 (3.8 mL) and cooled to 0 °C. Chloro-*N*,*N*-diisopropylamino-*β*-cyanoethylphosphine was then added (320 μL, 1.4 mmol, 1.5 equiv), and the mixture was stirred under N_2 while gradually warming to room temperature for 2 h. The excess chloridate was quenched by the addition of dry MeOH (0.5 mL), and the mixture was diluted into Et_3N/EtOAc (10 mL 1:9) and washed with ice-cold saturated sodium bicarbonate and brine. The organic layer was dried over Na_2SO_4 and concentrated under reduced pressure to give a tan foam. The residue was chromatographed on silica gel (eluting with a step gradient of 15−25% acetone in petroleum

(50) (a) Breslauer, K. J.; Frank, R.; Blöcker, H.; Marky, L. A. *Proc. Natl. Acad. Sci. U.S.A.* **1986**, *83*, 3746−3750. (b) Breslauer, K. J. *Thermodynamic Data for Biochemistry and Biotechnology*; Hinz, H.-J., Ed.; Springer-Verlag: Berlin, 1986; Chapter 15, pp 413−414. (c) Klump, H. H. *Biochemical Thermodynamics*; Jones, M. N., Ed.; Elsevier: New York, 1988; pp 100−144.

(51) Snell, F. D.; Snell, C. T. *Colorimetric Methods of Analysis*, 3rd ed.; Van Nostrand: New York, 1949; Vol. 2, p 671.

(52) Fiszer-Szafarz, B. *Anal. Biochem.* **1984**, *143*, 76−81.

(53) Plateau, P.; Guéron, M. *J. Am. Chem. Soc.* **1982**, *104*, 7310−7311.

(54) Blatt, N. B.; Osborne, S. E.; Cain, R. J.; Glick, G. D. *Biochimie* **1993**, *75*, 433−441.

ether) affording **3** (0.53 g, 71% yield, 1:1 mixture of diastereomers) as a white foam. TLC (25% acetone in petroleum ether) $R_f = 0.40$. ^{1}H NMR (360 MHz, CD_3CN) δ 1.02−1.18 (12 H, m, 2 NCH(C*H*$_3$)$_2$), 1.30 (9 H, s, C(C*H*$_3$)$_3$), 1.51−1.52 (3 H, d, 5-C*H*$_3$), 2.35−2.43 (2 H, m, 2′-*H*$_{a,b}$), 2.49−2.64 (2 H, m, OCH$_2$C*H*$_2$CN), 2.89 (2 H, t, $J = 7.3$ Hz, 8-*H*$_{a,b}$), 3.25−3.38 (2 H, m, 5′-*H*$_{a,b}$), 3.48−3.82 (4 H, m, OC*H*$_2$CH$_2$-CN, 2 NC*H*(CH$_3$)$_2$), 3.75 (6 H, s, 2 OC*H*$_3$), 4.05−4.15 (3 H, m, 4′-*H*, 7-*H*$_{a,b}$), 4.60−4.63 (1 H, m, 3′-*H*), 6.24−6.30 (1 H, m, 1′-*H*), 7.28−7.47 (13 H, m, Ar*H*), 7.50 (1 H, s, 6-*H*). ^{13}C NMR (90 MHz, CD_3-CN) δ 13.0 (5-*C*H$_3$), 20.9, 21.0 (OCH$_2$*C*H$_2$CN), 24.8, 24.8, 24.9 (NCH(*C*H$_3$)$_2$), 30.1 (C(*C*H$_3$)$_3$), 37.2 (8), 40.1, 40.2 (N*C*H(CH$_3$)$_2$), 41.3 (7), 43.9, 44.1 (2′), 48.4 (*C*(CH$_3$)$_3$), 55.9 (O*C*H$_3$), 59.3, 59.5 (O*C*H$_2$-CH$_2$CN), 64.1 (5′), 64.3 (3′), 85.8, 85.8 (1′), 86.1, 86.2 (4′), 87.4 (O*C*(Ph)$_3$), 110.5, 110.6 (5), 114.1, 128.0, 128.9, 129.0, 129.0, 131.1 (Ar.), 135.1, 135.2 (6), 136.6, 136.6, 136.7, 145.9 (Ar.), 151.7 (2), 159.8 (Ar.), 164.0 (4). ^{31}P NMR (202 MHz, CD_3CN) δ 145.78. IR (KBr) 2966, 2242, 1705, 1669, 1647, 1510, 1465, 1448, 1252, 1179, 1082, 1034, 1008, 977, 829 cm^{-1}. FAB MS (3-NBA) *m/z* 893 ($M^+ + 1$). Anal. Cacld for $C_{46}H_{62}N_4O_8PS_2$: C, 61.85; H, 6.90; N, 6.27. Found: C, 61.98; H, 6.64; N, 6.11.

5′-*O*-(4,4′-Dimethoxytrityl)-3′-*O*-succinyl-*N*^{3}-(ethyl)thymidine *tert*-Butyl Disulfide (4). Compound **2** (1.03 g, 1.49 mmol) and 4-(dimethylamino)pyridine (91 mg, 0.75 mmol, 0.5 equiv) were dissolved in pyridine (6 mL) and succinic anhydride (157 mg, 1.56 mmol, 1.05 equiv) was added to the solution as a solid over 5 min. The mixture was stirred under N_2 at 45 °C for 18 h after which the solution was diluted with CH_2Cl_2 and washed with ice-cold 10% citric acid, saturated sodium bicarbonate, and brine. The organic layer was dried over Na_2SO_4 and concentrated under reduced pressure to give a yellow foam. The residue was chromatographed on silica gel (eluting with a step gradient of 0−10% MeOH in 4:6 acetone:petroleum ether) affording **4** (0.90 g, 76% yield) as a white foam. TLC (4:5:1 acetone: petroleum ether:MeOH) $R_f = 0.47$ ^{1}H NMR (360 MHz, CD_3CN) δ 1.30 (9 H, s, C(C*H*$_3$)$_3$), 1.45 (3 H, s, 5-C*H*$_3$), 2.37−2.43 (2 H, m, 2′-*H*$_{a,b}$), 2.55 (4 H, bs, C*H*$_2$C*H*$_2$CO$_2$H), 2.89 (2 H, t, $J = 7.3$ Hz, 8-*H*$_{a,b}$), 3.30 (1 H, dd, $J = 2.9$, 10.6 Hz, 5′-*H*$_a$), 3.37 (1 H, dd, $J = 3.5$, 10.6 Hz, 5′-*H*$_b$), 3.75 (6 H, s, 2 OC*H*$_3$), 4.07−4.09 (1 H, m, 4′-*H*), 4.12 (2 H, t, $J = 7.3$ Hz, 7-*H*$_{a,b}$), 5.36−5.38 (1 H, m, 3′-*H*), 6.29 (2 H, dd, $J = 6.6$, 8.1 Hz, 1′-H), 6.84−7.43 (13 H, m, Ar*H*), 7.49 (1 H, s, 6-*H*). ^{13}C NMR (90 MHz, CD_3CN) δ 12.9 (5-*C*H$_3$), 30.1 (C(*C*H$_3$)$_3$), 37.2 (8), 38.1 (2′), 41.4 (7), 48.4 (*C*(CH$_3$)$_3$), 55.9 (O*C*H$_3$), 64.6 (5′), 75.9 (3′), 84.6 (1′), 86.1 (4′), 87.6 (O*C*(Ph)$_3$), 110.9 (5), 114.2, 128.0, 129.0, 131.0 (Ar.), 135.0 (6), 136.5, 136.7, 145.8 (Ar.), 151.8 (2), 159.8 (Ar.), 164.0 (4), 172.4 (*C*O$_2$CH$_2$CH$_2$CO$_2$H), 173.0 (CO$_2$CH$_2$CH$_2$*C*O$_2$H). IR (KBr) 3327, 2929, 2851, 1741, 1707, 1668, 1627, 1611, 1578, 1246, 1175, 1158, 828 cm^{-1}. FAB MS (3-NBA) *m/z* 792 ($M^+ + 1$).

5′-*O*-(4,4′-Dimethoxytrityl)-3′-*O*-succinyl-(*p*-nitrophenyl ester)-*N*^{3}-(ethyl)thymidine *tert*-Butyl Disulfide (5). Compound **4** (0.76 g, 0.96 mmol) was dissolved in CH_2Cl_2 (4 mL) cooled to 0 °C, and *N,N*-dicyclohexylcarbodiimide (198 mg, 0.96 mmol, 1.0 equiv) was added as a solid in one portion. The mixture was stirred under N_2 at 0 °C for 5 min after which *p*-nitrophenol (134 mg, 0.96 mmol, 1.0 equiv) was added. The reaction was stirred under N_2 at 0 °C for 4 h after which the *N,N*-dicyclohexylurea that had precipitated during the reaction was filtered through Celite. The Celite was washed with ice-cold CH_2Cl_2, and the organic layer was concentrated under reduced pressure. The residue was chromatographed on silica gel (eluting with a step gradient of 25−50% EtOAc in petroleum ether) affording **5** (0.52 g, 59% yield) as a white foam. TLC (1:1 EtOAc:petroleum ether) $R_f = 0.62$. ^{1}H NMR (360 MHz, CD_3CN) δ 1.29 (9 H, s, C(C*H*$_3$)$_3$), 1.47 (3 H, s, 5-C*H*$_3$), 2.38−2.44 (2 H, m, 2′-*H*$_{a,b}$), 2.70−2.91 (6 H, m, 8-*H*$_{a,b}$, C*H*$_2$C*H*$_2$CO$_2$H), 3.30 (1 H, dd, $J = 3.1$, 10.5 Hz, 5′-*H*$_a$), 3.37 (1 H, dd, $J = 3.7$, 10.5 Hz, 5′-*H*$_b$), 3.74 (6 H, s, 2 OC*H*$_3$), 4.08−4.14 (3 H, m, 4′-*H*, 7-*H*$_{a,b}$), 5.40−5.44 (1 H, m, 3′-*H*), 6.30 (1 H, dd, $J = 6.1$, 8.3 Hz, 1′-*H*), 6.84−8.25 (17 H, m, Ar*H*), 7.48 (1 H, s, 6-*H*). ^{13}C NMR (90 MHz, CD_3CN) δ 12.9 (5-*C*H$_3$), 29.8 (CO$_2$*C*H$_2$CH$_2$CO$_2$PNP), 30.0 (CO$_2$CH$_2$*C*H$_2$CO$_2$PNP), 30.1 (C(*C*H$_3$)$_3$), 37.2 (8), 38.1 (2′), 41.4 (7), 48.4 (*C*(CH$_3$)$_3$), 55.9 (O*C*H$_3$), 64.6 (5′), 76.2 (3′), 84.6 (1′), 86.1 (4′), 87.6 (O*C*(Ph)$_3$), 110.9 (5), 114.1, 123.8, 126.2, 128.0, 129.0, 131.0 (Ar), 134.9 (6), 136.5, 136.6, 145.8 (Ar.), 151.8 (2), 159.8 (Ar.), 163.9 (4), 171.6 (*C*O$_2$CH$_2$CH$_2$CO$_2$PNP), 172.6 (CO$_2$CH$_2$CH$_2$*C*O$_2$PNP). IR (KBr) 3329, 2932, 2853, 1740, 1705, 1669, 1647, 1526, 1510, 1347, 1252, 1176, 1121, 829 cm^{-1}. FAB MS (3-NBA) *m/z* 914 ($M^+ + 1$). Anal. Cacld for $C_{47}H_{51}N_3O_{12}S_2$: C, 61.68; H, 5.63; N, 4.59. Found: C, 61.28; H, 5.52; N, 4.37.

5′-*O*-(4,4′-Dimethoxytrityl)-3′-*O*-succinyl-(CPG)-*N*^{3}-(ethyl)thymidine *tert*-Butyl Disulfide (6). Amino-substituted CPG (0.51 g, 500 Å, 120/200 mesh, 100.1 μmol/g NH_2 substitution) and Et_3N (95 μL, 0.68 mmol, 2.0 equiv) were suspended in DMF (3.4 mL). The resin was swirled for several minutes after which active ester **5** (0.31 g, 0.34 mmol, 1.0 equiv) was added to the resin. The resin was swirled (the mixture instantaneously became bright yellow) under N_2 at room temperature for 18 h after which the support was isolated by filtration and washed with DMF, MeOH, Et_2O, and dried overnight under reduced pressure. The remaining amino groups on the CPG were capped by suspending the resin in pyridine (2.5 mL) and 4-(dimethylamino)-pyridine (0.3 mg, 2 μmol, 0.1 equiv) followed by the addition of acetic anhydride (0.3 μL, 3 μmol, 0.01 equiv). The resin was swirled under N_2 at room temperature for 30 min after which the support was isolated by filtration and washed with pyridine, MeOH, Et_2O, and dried overnight under reduced pressure. The amount of **6** loaded was determined by release of the 5′-dimethoxytrityl cation as described by Schaller and co-workers and was usually 33 μmol/g.[28]

Nucleic Acids Synthesis. Solid-phase DNA synthesis was conducted on a Millipore Expedite 8909 DNA/RNA synthesizer using dA^{N-Bz}, dC^{N-Bz}, dG^{N-iBu}, and dT β-cyanoethyl-*N,N*-diisopropylamino phosphoramidites following the manufacturer's protocols. Average coupling efficiencies were >98.5%. HPLC was performed using either a Waters Associates model 600 chromatograph coupled to a Waters model 484 absorbance detector (260 nm) for peak detection or a Waters 510 chromatograph coupled to a Waters 441 absorbance detector (254 nm) for peak detection. Unless otherwise noted, purification of oligodeoxynucleotides was conducted using Vydac C_4 columns (4.6 × 250 mm for analysis, 1 mL/min and 7.9 × 250 mm for preparative runs, 4 mL/min) and triethylammonium acetate (TEAA; 0.05 M, pH 6.6) and CH_3CN as the mobile phases. All sequences were ion-exchanged into the sodium form prior to analysis by incubating the DNA in NaCl (4 M) overnight at 4 °C. The excess salts were removed by reversed-phase HPLC (step gradient of 100% H_2O−0% CH_3CN in 7 min to 80% H_2O-20% CH_3CN in 15 min). All sequences prepared following this protocol were >99% pure as judged by HPLC and denaturing PAGE (20% polyacrylamide gels (19:1) containing 8 M urea). Molar extinction coefficients (ϵ_{260}, M^{-1} cm^{-1}) were determined by phosphate analysis as described by Snell and Snell[51] and are 113,000 for I; 112 000 for II; 107 000 for III; 110 000 for IV; 242 000 for V; and 197 000 for VI.

***tert*-Butyl Protected Duplexes III and IV.** Support containing modified thymidine **6** (30 mg, 1 μmol) was loaded into an empty reaction cartridge and elongated to give the sequences shown in Figure 1 (the terminal trityl group was not removed). Amidite **3** was added through the 5-nucleotide port on the synthesizer in the last coupling step. After the synthesis was complete, the resin was removed from the reaction column and suspended in concentrated NH_4OH (0.5 mL). After 1 h the support was pelleted by centrifugation, and the supernatant was removed and washed with fresh NH_4OH (0.5 mL). After an additional 7 h at 55 °C the NH_4OH was removed *in vacuo*. The residue was dissolved in water (2 mL) and purified by reversed-phase HPLC (linear gradient of 80% TEAA−20% CH_3CN to 35% CH_3CN in 60 min for sequence III, or a linear gradient of 75% TEAA−25% CH_3-CN to 45% CH_3CN in 60 min for sequence IV). Retention times are 22.5 min for III and 26.1 min for IV. The fractions that contained the product were pooled, and the solvent was removed *in vacuo*. The 5′-trityl group was removed by treating the DNA with 80% AcOH (1 mL). After 20 min the reaction was quenched with EtOH (0.2 mL), and the solvent was removed *in vacuo*. The *tert*-butyl protected modified sequences were purified by reversed-phase HPLC (linear gradient of 95% TEAA−5% CH_3CN to 25% CH_3CN in 60 min for III, or a linear gradient of 85% TEAA−15% CH_3CN to 30% CH_3CN in 60 min for IV) to give 2.59 mg (0.68 μmol, 68% yield) of III or 2.77 mg (0.71 μmol, 71% yield) of IV. Retention times are 27.8 min for III and 30.7 min for IV.

Cross-Linked Duplexes V and VI. The reduction of the *tert*-butyl protected dodecamers was performed by dissolving the DNA in buffer (0.1 M NaH_2PO_4, [DNA] = 2 mM, pH 8.3) containing DTT (200 equiv)

and incubating at 4 °C while monitoring the reaction via reversed-phase HPLC. After 18 h, the reduction was complete, and the reduced sequences were purified away from excess DTT by reversed-phase HPLC (linear gradient of 95% TEAA−5% CH_3CN to 25% CH_3CN in 60 min for III, or linear gradient of 90% TEAA−10% CH_3CN to 25% CH_3CN in 60 min for IV). Retention times are 17.4 min for reduced III and 28.2 min for reduced IV. The solvent was removed *in vacuo*, and the DNA was dissolved in buffer (1 mM NaH_2PO_4; [DNA] = 2 mM, [NaCl] = 0.1 M, pH 8.3) and vigorously stirred for 18 h exposed to the atmosphere. Every 3 h an aliquot (3 μL) was removed from the reaction mixture and tested for the presence of free thiol groups with Ellman's reagent. After 18 h, a negative test was observed, and the mixture was then acidified with AcOH to pH 3 and the cross-linked duplexes were purified by reversed-phase HPLC (linear gradient of 95% TEAA−5% CH_3CN to 20% CH_3CN in 60 min) to give 3.03 mg (0.41 μmol, 41% yield) of V and 2.06 mg (0.55 μmol, 55% yield) of VI**.** Retention times are 24.8 min for V and 29.3 min for VI.

Nucleoside Composition Analysis. DNA samples (0.4 OD_{260} U) were dissolved in water (to 24 μL). Dephosphorylation buffer (4 μL of 500 mM TRIS-HCl, 1 mM EDTA, pH 8.5), calf intestine alkaline phosphatase (6 μL, 6 U), and snake venom phosphodiesterase from *Crotalus durissus* (6 μg, to a total volume of 40 μL) were added, and the mixture was incubated at 37 °C for 24 h. Aliquots of the reaction mixture (15 μL) were filtered through an Amicon Microcon-3 filter to remove the protein and analyzed by HPLC (linear gradient of 98% TEAA−2% CH_3CN to 5% CH_3CN in 12 min, linear gradient to 10% CH_3CN in 8 min, and then linear gradient to 70% CH_3CN in 20 min) using a Phenomenex μBondaclone C_{18} column (3.8 × 300 mm, 1 mL/min) and peaks quantitated via a Shimadzu C-R6A integrator using nucleoside extinction coefficients[1b] (ϵ_{254}, M^{-1} cm^{-1}) of 13 300, for dA; 6300 for dC; 13 000 for dG; 6600 for T; 5700 for **T*$_{tBu}$**; and 10 500 for **T*$_2$**. Retention times (min) are 4.6 for dC; 11.2 for T; 10.7 for dG; 17.6 for dA; 31.5 for **T*$_2$**; 36.7 for **T*$_{tBu}$**.

Disulfide Reduction Studies: HPLC. Mononucleosides **T*$_{tBu}$** and **T*$_2$** (1.0 nmol) and dodecamers IV and V (1.0 nmol and 0.5 nmol, respectively) were incubated in buffer (50 μL, 10 mM TRIS-HCl, 1 mM EDTA, pH 8.3) with various concentrations of DTT (0.1, 1.0, and 5.0 mM). Aliquots (4 μL) were quenched with AcOH (0.5 μL of a 0.1 M solution) at the indicated times and then quickly chilled on ice. The samples were then analyzed by reversed-phase HPLC (C_{18} column for monomers and C_4 column for oligonucleotides) by peak integration of the remaining starting material relative to an unmodified standard. Apparent half-lives were calculated based on remaining starting material using exponential curve fitting (assuming second-order kinetics). Error in the apparent half-lives is ±10%.

Disulfide Reduction Studies: Gel Electrophoresis. Sequence VI (20 μg/mL) was incubated in buffer (40 μL, 10 mM TRIS-HCl, 1 mM EDTA, pH 8.3 or 7.0) with various reductant concentrations (DTT or BME) at 25 °C. Aliquots (4 μL) were withdrawn and quenched with AcOH (0.5 μL of a 0.1 M solution) at the indicated times and then quickly chilled on ice. The DNA was electrophoresed on a 20% nondenaturing polyacrylamide gel (10 × 10 cm × 0.75 mm) and were visualized with Stains-All.[52] The bands were quantified by laser densitometry and half-lives were calculated as described for the HPLC reduction experiments. Error in the apparent half-lives is ±10%.

CD Spectroscopy. CD spectra were measured on an AVIV 62DS spectrometer equipped with a thermoprogrammable peltier with a step size of 0.5 nm, bandwidth of 1.5 nm, and signal averaging time of 1.0 s. Each scan was repeated five times with the resultant average plot smoothed using manufacturers protocols ($\delta/\delta^2 \leq 2.25$). For each sample, CD measurements were performed in 0.1-cm long self-masking cuvettes and DNA concentrations were determined based on dynode voltage at 260 nm.

NMR Spectroscopy. NMR spectra of oligonucleotide samples were measured on a Bruker AMX 500 spectrometer. DNA samples were dissolved in buffer (10 mM NaH_2PO_4; 500 μL, 90% H_2O/10% D_2O, pH 7.0) to a final concentration of 2.0 mM. The samples were heat-denatured and slowly renatured prior to analysis. The carrier frequency was centered on the water resonance, which was suppressed using a jump and return pulse sequence for all spectra.[53] All spectra were referenced to the water resonance. The NOESY spectra were measured at both 10 and 30 °C with a mixing time of 200 ms. 640 t_1 increments of 4096 complex points were collected. The spectral width in both dimensions was 10 000 Hz. The data was transferred to a Silicon Graphics workstation and processed using the FELIX software (Biosym Technologies). All spectra were convoluted in the time dimension in order to reduce the intensities of the water resonance. The exchangeable protons were assigned as previously described.[21e]

UV Denaturation Experiments. UV spectra were measured on a Cary 3 spectrophotometer equipped with a Varian Peltier. Prior to melting, the solutions were heated to 98 °C and then allowed to cool at a constant rate of 3 °C/min to 5 °C. After equilibration for 30 min, the absorbance was monitored at 259 nm while heating to 98 °C at a rate of 0.5 °C/min in 0.1-cm long self-masking cuvettes. DNA concentrations were based on extrapolating the upper baseline to 90 °C using extinction coefficients given above. The optical melting transitions were translated into fraction of initial state (α) versus temperature using the sloping baselines technique.[37] In the case of the non-self-complementary sequence III, a symmetry factor of Rln(4) is included in the van't Hoff enthlapy (H_{vH}) analysis. For the monomolecular hairpin V, the melting temperature and the van't Hoff enthalpy were determined using nonlinear regression analysis as previously described.[54] Melting temperatures are defined as the temperature where α is equal to 0.5 and have a variance of ±1.0 °C.

DSC Denaturation Experiments. Apparent excess heat capacity (ΔC_p) versus temperature profiles for oligonucleotides I, II, V, and VI were measured using either a Microcal MC2 (Microcal, Amherst, MA) or DS93 (Johns Hopkins University, Baltimore, MD) differential scanning calorimeter. Oligonucleotide solutions ranging from 0.1 to 0.9 mM total strand concentration in 100 mM NaCl, 10 mM NaH_2PO_4, pH 7.0 buffer were scanned repeatedly from 5 to 105 °C (MC2) or 120 °C (DS93) using a constant heating rate of 1 °C/min and analyzed as previously described.[21c] For a given oligonucleotide, the resulting enthalpy and entropy values determined using the two calorimeters were within 5%, which reflects the uncertainty in the measurements.

^{32}P Labeling. DNA samples (7 pmol) were end-labeled in reaction buffer (10 μL, 100 mM TRIS-HCl, 10 mM $MgCl_2$, 0.1 mM EDTA, 5% glycerol, pH 7.5) containing [γ^{32}P] ATP (10 μCi, 3,000 Ci/mmol) and T4 polynucleotide kinase (10 U). Reactions were incubated at 37 °C for 1.5 h then purified by nondenaturing PAGE on 20% polyacrylamide gels (10 × 10 cm x 0.75 mm). Gel slices were soaked in water (250 μL) at 4 °C overnight, and the radiolabeled DNA samples were separated from the gel fragments through a Micropure filter.

Restriction Endonuclease Digestion. DNA samples (3 pmol, 50 000 cpm) were diluted in buffer (4.5 μL, 50 mM TRIS-HCL, 100 mM NaCl, 10 mM $MgCl_2$, 1 mM dithioerythritol, pH 7.5), and *Eco*RI (0.5 μL, 5 U) was added. The reactions were incubated for 1 h at 37 °C and quenched with EDTA (0.5 μL of a 0.5 M solution), and the fragments were separated by nondenaturing PAGE on 20% polyacrylamide gels (10 × 10 × 0.5 cm). The gels were autoradiographed for 12 h at −78 °C and analyzed using a Molecular Dynamics Personal Laser Densitometer running the IMAGEQUANT software. Note that when these experiments are conducted without dithioerythritol being present in the enzyme incubation buffer, similar results to those presented in Figure 6 are obtained.

Exonuclease Resistance. DNA samples (0.25 mM) were incubated in buffer (to a total volume of 20 μL, 50 mM TRIS-HCl, 100 mM NaCl, 1 mM $MgCl_2$, pH 9.2) with snake venom phosphodiesterase from *Crotalus durissus* (1 U/10 nmol DNA) at 37 °C. Aliquots (2 μL) were withdrawn and quenched with EDTA (0.5 μL of a 0.5 M solution) at the indicated times and chilled on ice. The DNA was analyzed and quantified as described above. Error in the apparent half-lives is ±5%.

Acknowledgment. Supported by NIH Grant GM 52831. G.D.G. is the recipient of a National Arthritis Foundation Arthritis Investigator Award, an American Cancer Society Junior Faculty Research Award, a National Science Foundation Young Investigator Award, a Camille Dreyfus Teacher-Scholar Award, and a Research Fellowship from the Alfred P. Sloan Foundation.

JA962386C